ZAKIR HUSSAIN COLLEGE OF ENGINEERING AND TECHNOLOGY

AERODYNAMIC & STRUCTURAL ANALYSIS OF WIND TURBINE BLADE

SUPERVISOR

Mr. Ateeb Ahmad Khan

Assistant Professor

Department of Mechanical Engineering

Presented By

Ashneet Pal Singh	16MEB353
Mohd Tauseef Raza	16MEB378
Mohd Rashid Siddiqui	16MEB258

ABSTRACT

This project considers the deformation due to the aerodynamic loading of a wind turbine blade by performing a steady-state 1-way FSI (Fluid-Structure Interaction) analysis. Part 1 of this project uses ANSYS Fluent to develop the aerodynamic loading on the blade. In part 2, the pressures on the wetted areas of the blade are passed as pressure loads to ANSYS Mechanical to determine stresses and deformations on the blade. Then the work explores to validate the strength of the blade and to compare analyze for five different materials like Structural Steel, Epoxy Carbon, S-glass, E-glass & Aluminium alloy & select the best material out of these for the wind turbine blade.

The ultimate objective of the project is to analyze the various parameters involved in designing of the wind turbine blades through the structural analysis and to calculate an optimum blade shape, for the procedure begins with the choice of airfoils characteristics. Then an initial wind blade design is determined using blade element momentum. The blade plays a pivotal role because it is the most important part of the energy absorption system. Practical horizontal axis wind turbine (HAWT) designs use airfoils to transform the kinetic energy in the wind into useful energy and it has to be designed carefully to enable to absorb energy with its greatest efficiency. There are many factors for selecting a profile. One significant factor is the chord length and twist angle which depend on various values throughout the blade. Computational Fluid Dynamics (CFD) are used for wind turbines airfoils static structural analysis. This differs from the traditional aerospace design process since the lift-to-drag ratio is the most important parameter and the angle of attack is large. CFD simulations are performed with the incompressible Reynolds Averaged Navier–Stokes equations in steady state using a one equation turbulence model. The aim of the analysis is to validate the strength of the blade and compare the above materials to select the best material for the wind turbine blade.

TABLE OF CONTENTS

LIST OF TABLES

LIST OF FIGURES

Chapter 1 : Introduction

1.1. Introduction

Blade is the key component to harness wind energy. In this project, computational fluid dynamics analysis is conducted on a wind turbine blade with NREL S818, S825 and S826 airfoil design. The project conducts the analysis of an existing wind turbine blade [1]. The blade optimization is carried out by considering parameter like shapes of airfoil profile, stresses and deformation on blade. When designing a wind turbine, the aim is to attain the highest possible power output under particular atmospheric conditions and this depends on the shape of the blade as well as on its material [2]. The utilization of the energy in the winds requires the development of devices which convert that energy into more useful forms. This is typically accomplished by first mechanically converting the linear velocity of the wind into a rotational motion by means of a windmill and then converting the rotational energy of the windmill blades into electrical energy by using a generator or alternator. For purposes here, we can thus view windmill as a mechanical device for extracting some of the kinetic energy of the wind and converting it into the rotational energy of the blade motion. This is accomplished, in detail, by having the blades oriented at some angle to the wind so that the wind blowing past the blades exerts an aerodynamic force on them and there by causes them to rotate. The dynamic and mechanical properties of a wind turbine can be modified by changing the composite material of the blade [3]. Hence emphasis is given on the material of the blade. The results of analysis of different material are compared to evaluate the best possible one suited for practical application.

1.2. Windmill Blade

Among all the parts of wind turbines (blades, hub, gearbox, generator, nacelle, tower...), composite materials are used in blades and nacelles [4]. The main requirements to nacelles, which provide weather protection for the components, are the low weight, strength and corrosion resistance. Typically, nacelles are made from glass fiber composites. Increasing the reliability and lifetime of wind blades is an important problem for the developers of wind turbines. The wind turbine blades are built as follows. A blade consists of two faces (on the suction side and the pressure side), joined

together and stiffened either by one or several integral (shear) webs linking the upper and lower parts of the blade shell or by a box beam (box spar with shell fairings). The box beam inside the blade is adhesively joined to the shell. Figure 3.4 shows the schema of the section of the blade. Wind turbine blades are complex structures whose design involves the two basic aspects of

- Selection of the aerodynamic shape
- Structural configuration
- Material selection (to ensure that the defined shape is maintained for the expected life)
- Density of Blade Material

Figure 1: Modern Wind Turbine Blade

The general considerations in the design of wind turbine blade are:

1.2.1. Theoretical Maximum Efficiency

High rotor efficiency is desirable for increased wind energy extraction and should be maximized within the limits of affordable production [5]. Energy (P) carried by moving air is expressed as a sum of its kinetic energy:

$$P = \frac{1}{2}\rho A V^3 \qquad \textbf{(1)}$$

where,

ρ = Air Density; A = Swept Area; V = Air Velocity

A physical limit exists to the quantity of energy that can be extracted, which is independent of design. The energy extraction is maintained in a flow process through the reduction of kinetic energy and subsequent velocity of the wind. The magnitude of energy harnessed is a function of the reduction in air speed over the turbine. 100% extraction would imply zero final velocity and therefore zero flow. The zero flow scenario cannot be achieved hence all the winds kinetic energy may not be utilized. This principle is widely accepted and indicates that wind turbine efficiency cannot exceed 59.3%. This parameter is commonly known as the power coefficient Cp, where max C_p = 0.593 referred to as the Betz limit [6]. The Betz theory assumes constant linear velocity. Therefore, any rotational forces such as wake rotation, turbulence caused by drag or vortex shedding (tip losses) will further reduce the maximum efficiency. Efficiency losses are generally reduced by:

- Avoiding low tip speed ratios which increase wake rotation
- Selecting airfoils which have a high lift to drag ratio
- Specialized tip geometries.

1.2.2. Angle of Twist

The lift generated by an airfoil section is a function of the angle of attack to the inflowing air stream. The inflow angle of the air stream is dependent on the rotational speed and wind speed velocity at a specified radius. The angle of twist required is dependent upon tip speed ratio and desired airfoil angle of attack. Generally the airfoil section at the hub is angled into the wind due to the high ratio of wind speed to blade radial velocity. In contrast the blade tip is likely to be almost normal to the wind. The total angle of twist in a blade maybe reduced simplifying the blade shape to cut manufacturing costs. However, this may force airfoils to operate at less than optimum angles of attack where lift to drag ratio is reduced [7]. Such simplifications must be well justified considering the overall loss in turbine performance.

1.2.3. Angle of Attack

The Angle of Attack is the angle at which relative wind meets an aerofoil. On an aerofoil such as one on a wind turbine, it is the angle between the chord line and the relative wind vector [8].

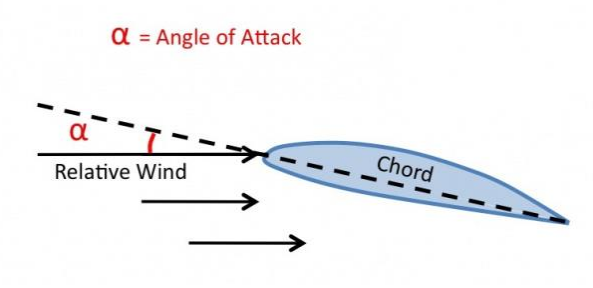

Figure 2: Angle of Attack

A number of terms are used to characterize an airfoil. The mean camber line is the locus of points halfway between the upper and lower surfaces of the airfoil. The most forward and rearward points of the mean camber line are on the leading edge and trailing edges, respectively. The straight line connecting the leading and trailing edges is the chord line of the airfoil, and the distance from the leading to the trailing edge measured along the chord line is designated as the chord of the airfoil. The thickness is the distance between the upper and lower surfaces, also measured perpendicular to the chord line. Finally, the angle of attack αis defined as the angle between the relative wind and the chord line.

Chapter 2 : Literature Review

2.1. Literature Review

Table 1: Literature Review

S.No	Title	Author	Work Done
1	Highway Windmill	R.Sathyanarayanan, C.Girira,MPrasath,S.Muthamizh,K.T.Gopinath	The j-type blade design rules out savonius design in high power energy generation & it has both the c-type design & aerodynamic wing design fused together forming an hybrid model shape , so that the blade acts on drag & lift theory of wind turbine for a normal air pressure the mechanical power produced will be much higher as compared to the other design types [9]
2	Experimental comparison study for Savonius Wind Turbine of Two or Three Blades at Low Wind Speed	Mohammed Hadi Ali	It was observed from the measured & calculated results that the two blades savonius wind turbine is more efficient , it has higher power coefficient under the same efficient , it has higher power coefficient under the same turbine . The reason is that increasing the number of blades will increase the drag surfaces against the wind air flow & causes to increase the reverse torque & leads to decrease the net torque working on the blades of savonius wind turbine. [10]
3	Design procedure for Lenz type vertical axis wind turbine for urban domestic application	Himmatsinh P . Gohil , Prof. ST Patel	From this paper one can learn a design procedure for latest invented Lenz VAWT . From the design calculation & based on previous research data in related domain , basic design parameters of Lenz type VAWT is derived which are tip speed ratio , wing dimensions etc. [11]

4	Wind turbine blade design	Peter J .Scubel & Richard J	Detail review of the current state of art for wind turbine blade design was presented including the aero foil section & optimal attack angle , maximum efficiency , propulsion, practical efficiency , HAWT blade design & blade loads [1]
5	Structural analysis of composite wind turbine	Akhil P.Matthew,Atul S , Barath P, Rakesh S	Modelling of wind turbine in Catia v5 & analyzed for five different materials like structural steel , epoxy , carbon , S-glass , E-glass , aluminium alloys. Then the work explores the finite element analysis for turbine blades using ANSYS software . Aim was to select the best material for the wind turbine blade [3]
6	Model validation & structural analysis of a small wind turbine blade	Pabut O,Allikash G,Herranen H,Talalaev R & Vene K	Validated a simplified finite element analysis(FEA) model for a glass fiber reinforced plastic(GFRP) wind turbine blade Experimental validation of the virtual model was performed on manufactured blade subject via bending test [12]

Chapter 3 : Methodology

3.1. Problem Specification

This project considers the deformation due to aerodynamic loading of a wind turbine blade by performing a steady-state 1-way FSI (Fluid-Structure Interaction) analysis. Part 1 of the tutorial uses ANSYS Fluent to develop the aerodynamics loading on the blade. In part 2, the pressures on the wetted areas of the blade are passed as pressure loads to ANSYS Mechanical to determine stresses and deformations on the blade.

The blade is 43.2 meters long and starts with a cylindrical shape at the root and then transitions to the airfoils S818, S825 and S826 for the root, body and tip, respectively [13]. This blade also has pitch to vary as a function of radius, giving it a twist and the pitch angle at the blade tip is 4 degrees. This blade was created to be similar in size to a GE 1.5XLE turbine.

The blade is made out of an orthotropic composite material, it has a varying thickness and it also has a spar inside the blade for structural rigidity. These specs, which are important for the FEA simulation, are described in more detail in Part 2 of the project.

The turbulent wind flows towards the negative z-direction (into the page on the above diagram) at 12 m/s which is a typical rated wind speed for a turbine this size. This incoming flow is assumed to make the blade rotate at an angular velocity of -2.22 rad/s about the z-axis (the blade is thus spinning clockwise when looking at it from the front, like most real wind turbines).

3.2. Modelling The Turbine Blade

The analysis of the blade in an analytical fashion yields useful first-pass results about stresses and moments, which is useful in determining basic strength and material requirements. This type of analytical analysis, though useful, is insufficient to properly evaluate the full wind turbine blade.

Accordingly, we sought to use 1-way FSI to more accurately capture the loads and stresses generated on the blade geometry by particular loading scenarios. This computational method allows for much greater flexibility in testing out various loads and blade geometries, allowing for an iterative approach to developing our turbine blade.

First, we began by selecting our airfoils. We decided to use the NREL S-series of airfoil [14]. These airfoils are in general somewhat thicker than the types typically seen on airplanes due to structural concerns, and are largely insensitive to roughness. As such, they are well suited for turbine blades.

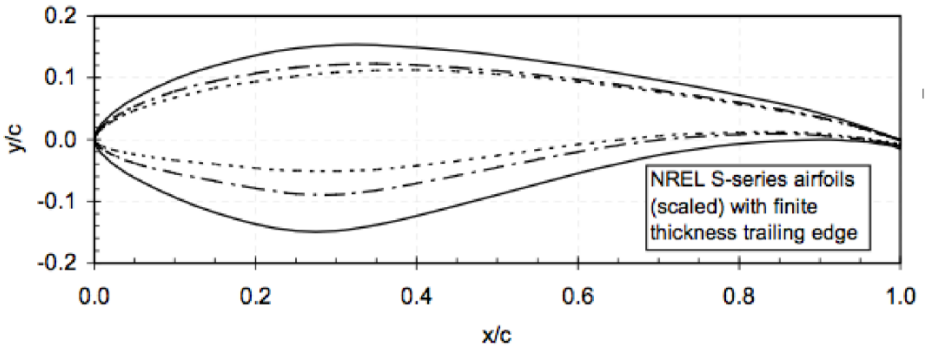

Figure 3: NREL Series Airfoils

The beginning of the blade is the circular hub section. This circular root transitions into the S818 airfoil, which then transitions to the S825 airfoil, which then transitions into the S826 airfoil used at the tip. The full blade geometry, including twist, span, and chord lengths, were determined through WT_Perf analysis and can be seen below [13].

Table 2: Data for Full Blade Geometry

S.No.	Radial Location, r (m)	Twist, α (°)	Chord Length, C (m)	Spar Location, C/4 (m)	NREL Airfoil
1	7.1	0	2.55	0.6375	S818
2	11.2	-5	3.1	0.775	
3	19.45	-13.1	2.7	0.675	S825
4	27.7	-15.8	2.1	0.525	
5	35.95	-19	1.5	0.375	S826
6	44.2	-20	1	0.25	

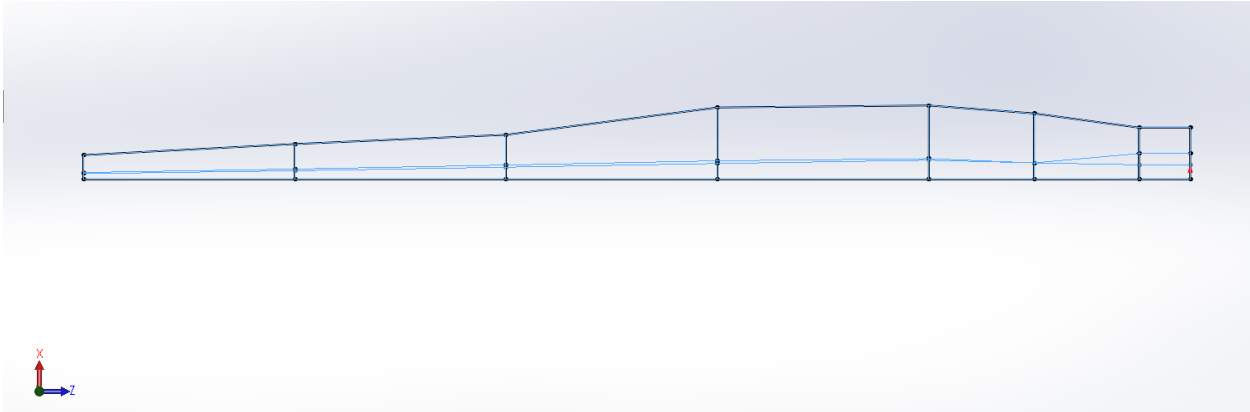

Figure 4: Blade sections at different radial locations

With the full blade geometry defined, we began the process of building the blade for our model. While it is possible to model and analyze a full wing using just ANSYS, we decided to model the blade using the SolidWorks CAD package instead due to familiarity with that program. As it is possible to import geometry directly from SolidWorks into ANSYS, this seemed to be the most efficient way to manage the creation of the blade.

In order to ensure maximum flexibility and computational efficiency within ANSYS, we designed the blade within SolidWorks as a lofted surface, which is analogous to building with ANSYS' shell elements. Blade design is essentially accomplished by pasting each airfoil element on a plane placed the appropriate distance from the turbine hub (the span distance). Then, using the surface loft command, it is possible to connect these various sketches into a single body, letting SolidWorks automatically generate the intermediate blade shape between each defined airfoil. To minimize unnecessary complications in the geometry, we lofted each section using the airfoil leading edge as the loft guide point.

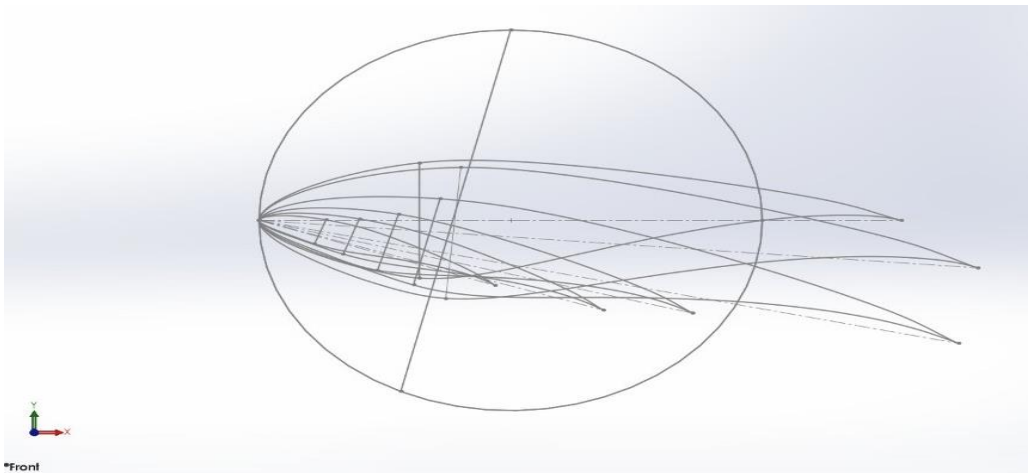

Figure 5: Various sections with a twist in blade

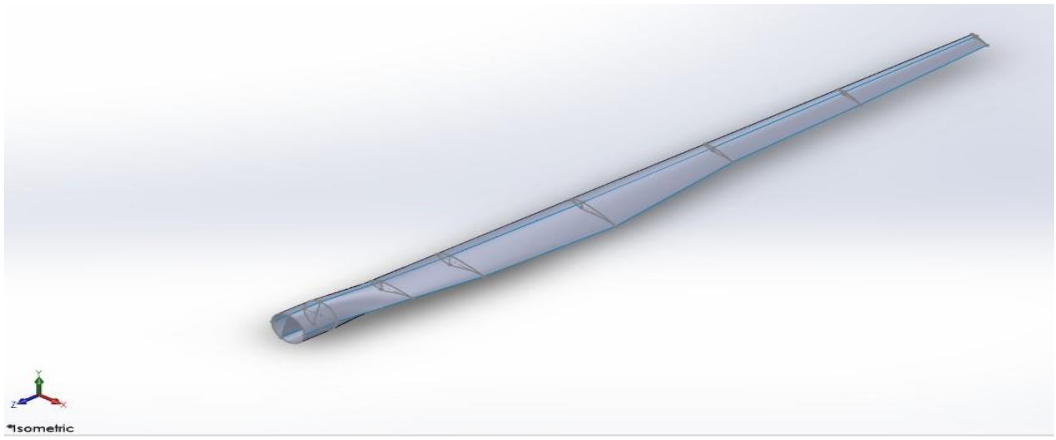

Figure 6: Full blade geometry

Additionally, it is important to note that the airfoil data had to be separated into the top and bottom sections for each airfoil. In our original attempt to create the blade we brought in each airfoil in its entirety and lofted the blade from these full airfoils, but we found this method yielded problems within ANSYS. The FEA package was not able to properly recognize defining features like the leading and trailing edges, which led to exceedingly complicated meshes or geometries that would not mesh at all, depending on the section analyzed. By separating the SolidWorks lofts into the top and bottom sections we essentially "created" these defining features, ensuring that ANSYS recognized the geometric constraints of the blade and yielded much simpler and efficient meshes.

3.3. CFD Methodology

In this section of the project, the blade geometry is imported, a mesh is created around the blade and the Fluent solver is then used to find the aerodynamics loading on the blade, the fluid

streamlines and the torque generated. We will use air at standard conditions (15 degree Celsius). Its density is 1.225 kg/m^3 and its viscosity is 1.7894e-05 kg/(m*s).

Using periodicity, we will simulate the flow around one blade and extrapolate the solution to two more blades in order to visualize the results for a 3 blade rotor. Here's a sneak peak of a particular result that you will obtain at the end of this project.

3.3.1. Mathematical Modelling

The governing equations are the continuity and Navier-Stokes equations. These equations are written in a frame of reference rotating with the blade. This has the advantage of making our simulation not require a moving mesh to account for the rotation of the blade.

The equations that we will use look as follows:

Conservation of mass:

$$\frac{\partial \rho}{\partial t} + \nabla . \rho \vec{v}_r = 0 \qquad \textbf{(2)}$$

Conservation of Momentum (Navier-Stokes):

$$\nabla . (\rho \vec{v}_r \vec{v}_r) + \rho (2\vec{\omega} \times \vec{v}_r + \vec{\omega} \times \vec{\omega} \times \vec{r}) = -\nabla p + \nabla . \tau_r'' \qquad \textbf{(3)}$$

Where $\vec{v}_r$ is the relative velocity (the velocity viewed from the moving frame) and $\vec{\omega}$ is the angular velocity.

Note the additional terms for the Coriolis force $(2\vec{\omega} \times \vec{v}_r)$ and the centripetal acceleration $(\vec{\omega} \times \vec{\omega} \times \vec{r})$ in the Navier-Stokes equations. In Fluent, we'll turn on the additional terms for a moving frame of reference and input $\vec{\omega} = -2.22\hat{k}$.

Important: We use the Reynolds Averaged form of continuity and momentum and use the SST k-omega turbulence model to close the equation set.

3.3.2. Boundary Conditions

We had model only 1/3 of the full domain using periodicity assumptions:

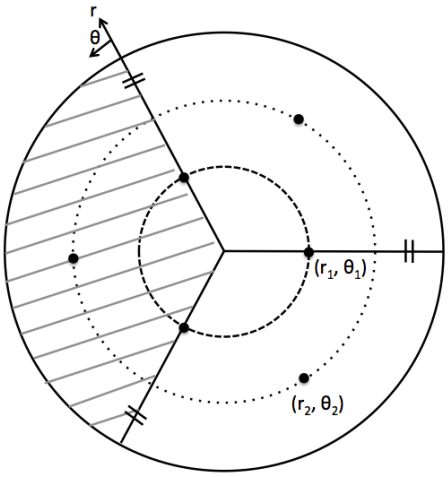

$$\vec{v}(r_1,\theta) = \vec{v}(r_1,\theta_1 - 120°n) \quad \text{For n = 1, 2, 3...}$$
$$= \vec{v}(r_1,240° - 120°(1)) = \vec{v}(r_1,120°)$$
$$= \vec{v}(r_1,240° - 120°(2)) = \vec{v}(r_1,0°)$$

$$\vec{v}(r_2,\theta) = \vec{v}(r_2,\theta_2 - 120°n) \quad \text{For n = 1, 2, 3...}$$
$$= \vec{v}(r_2,180° - 120°(1)) = \vec{v}(r_2,60°)$$

This therefore proves that the velocity distribution at theta of 0 and 120 degrees are the same. If we denote θ_1 to represent one of the periodic boundaries for the 1/3 domain and θ_2 being the other boundary, then $\vec{v}(r_i,\theta_1) = \vec{v}(r_i,\theta_2)$.

The boundary conditions on the fluid domain are as follow:

Inlet: Velocity of 12 m/s with turbulent intensity of 5% and turbulent viscosity ratio of 10

Outlet: Pressure of 1 atm

Blade: No-slip

Side Boundaries: Periodic

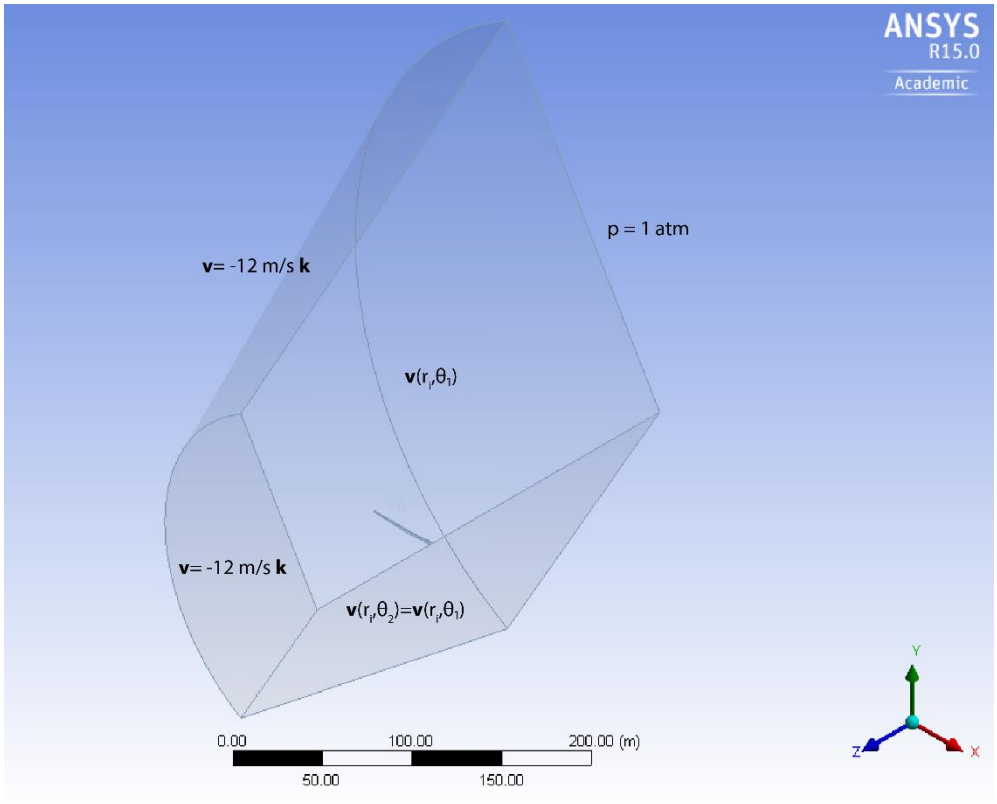

3.3.3. Hand Calculations of Expected Results

One simple hand-calculation that we can do now before even starting our simulation is to find theoretical wind velocity at the tip. We can then later compare our answer with what we get from our simulation to verify that they agree.

The velocity, v, on the blade should follow the formula

$$v = r \times \omega \quad \textbf{(4)}$$

Plugging in our angular velocity of -2.22 rad/s and using the blade length of 43.2 meters plus 1 meter to account for the distance from the root to the hub, we get

$$v = -2.22 \text{ rad/s } \hat{k} \text{ x } -44.2 \text{ m } \hat{i}$$

$$v = 98.12 \text{ m/s } \hat{j}$$

Additionally, by using the simple one-dimensional momentum theory, we can estimate the power coefficient which is the fraction of harnessed power to total power in the wind for the given turbine swept area. This analysis uses the following assumptions:

- The flow is steady, homogenous and incompressible.
- There is no frictional drag.

- There is an infinite number of blades.
- There is uniform thrust over the disc or rotor area.
- The wake is non-rotating.
- The static pressure far upstream and downstream of the rotor is equal to the undisturbed ambient pressure.

As mentioned in the problem statement, this blade is meant to resemble the GE 1.5 XLE wind turbine blade. The specification sheet of this turbine states the rated power of this turbine to be 1.5 MW, the rated wind speed to be 11.5 m/s and the rotor diameter to be 82.5 m.

Thus, at rated wind speed,

$$C_p = \frac{P_{rated}}{P_{wind}} = \frac{P_{rated}}{\frac{1}{2}\rho A V_{rated}^{\ 3}} = \frac{P_{rated}}{\frac{1}{2}(1.225)(\frac{\pi}{4}(82.5)^2)(11.5)^3} = 0.30$$

The resulting power coefficient of 0.30 is very reasonable. We will compare it to the power coefficient obtained from the simulation in the Verification & Validation section.

3.4. FEA Methodology

This section involves the solid mechanic's aspects of this wind turbine blade tutorial. The pressure load found using Fluent in Part 1 are imported in Mechanical and the stresses and deformations on the blade are subsequently determined.

The blade is composed of an outer surface and an inner spar. The thickness of the outside surface linearly decreases from 0.1 m at the root to 0.005 m at the tip. The spar has a similar thickness behavior with 0.1 m at its closest point to the root and 0.03 m at the tip. To sum up, here are the thickness specifications needed along with their location with respect to the global coordinate system (which represents the center of an imaginary hub and thus the center of rotation).

Table 3: Thickness Specifications of Wind Turbine Blade

SURFACE		SPAR	
X (m)	Thickness (m)	X (m)	Thickness (m)
-1	0.1	-3	0.1
-44.2	0.005	-44.2	0.03

These thicknesses are actually very close to what we would encounter on a real turbine.

Wind turbine blades are now made of composite materials to reduce the weight of these massive machines. Here we simplify the structural analysis by assuming that the composite material can be approximated by the following orthotropic material properties.

Density (kg/m^3)	1550
Young's Modulus-X (Pa)	1.1375E+11
Young's Modulus-Y (Pa)	7.583E+09
Young's Modulus-Z (Pa)	7.583E+09
Poisson's Ratio-XY	0.32
Poisson's Ratio-YZ	0.37
Poisson's Ratio-XZ	0.35
Shear Modulus-XY (Pa)	5.446E+09
Shear Modulus-YZ (Pa)	2.964E+09
Shear Modulus-XZ (Pa)	2.964E+09

Figure 7: Orthotrophic Composite Material Properties

These values are representative of composite properties found in real wind turbine blades.

3.4.1. Euler Bernoulli Beam Theory

The mathematical model for the wind turbine blade structural analysis is based on shell theory. The details of shell theory are quite involved and the mathematics is quite detailed. However, one can understand it conceptually in a straightforward fashion as an extension of Euler Bernoulli beam theory.

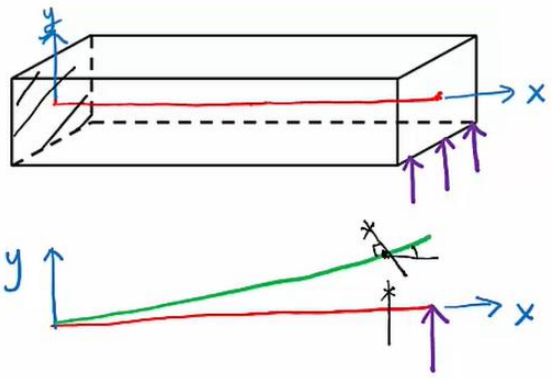

Figure 8: Euler Bernoulli Beam Theory

This figure above is a typical cantilever beam with a point load at the end & fixed at the other end. A beam is defined as a structure having one of its dimensions much larger than the other two. The axis of the beam is defined along that longer dimension, and a cross-section normal to this axis is assumed to smoothly vary along the span or length of the beam. To figure out the deformations in this beam we have to focus on the mid-line (colored in red). Under the influence of the given point load, mid line is going to deform as represented by green line. So any point on the mid-line is going to move in the y-direction (transverse direction) of the beam & the whole of cross-section of the beam will rotate about z-axis. That's one of the assumptions of Euler Bernoulli's beam theory. For small deformations the rotation angle of the cross-section will give the slope of the deformed mid-line curve. So by knowing the deformation of the mid-line, as well as the slope, we can back calculate where every point on the mid-line will move. So the whole problem reduces to figuring out the deformed state of the mid-line. By knowing the deformed state of the mid-line we can figure out what will the potential energy of the beam going to be because we know how every point is going to move, the displacement of every point from which we can calculate strains, and from the strains we can calculate the stresses based on the properties, and from that, the potential energy so we need to find the deform midline such that the potential energy is minimized.

Generally, Euler-Bernoulli beam theory is implied in ANSYS to analyze a cantilever beam. In terms of the wind turbine blade, the mathematical details are very complex in applying the shell theory to that particular example. However, we have a fancy calculator ANSYS at our disposal that will take care of the mathematical details and so we can focus on the physical principles on which the mathematical model is based and the assumptions embedded in that mathematical model.

3.4.2. Plate Theory

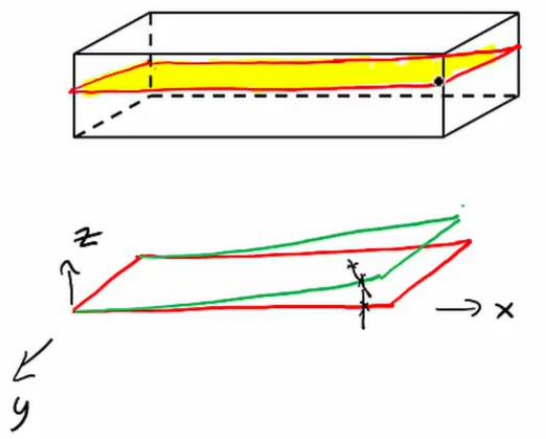

Figure 9: Plate Theory

Plate theory is a successive form of Euler-Bernoulli's theory. In this theory, instead of focusing on the mid-line, we focus on how the mid-surface is going to deform. in plate theory we saw that we focus on the mid surface, and how that mid surface is going to deform under the influence of the load, assuming that normals will remain normal at every point on the mid surface. Under the influence of the load the whole mid surface is going to deform like the one shown in the figure

above. While the deformation of the plane, the normal will still remain normal. So instead of saying that the cross section rotates together as a whole, the normal rotate together. For knowing how each point on the mid surface moves normal to itself, we need to know the rotation about x, y, and z axis, i.e. θ_x, θ_y and θ_z, respectively. This gives the displacement and rotations of the mid surface and how every point within the beam moves. By knowing the deformed surface we can find out the potential energy of the structure. By knowing the thickness of the beam we can find the strains. And, from the strains we can find the stresses by knowing the material properties. So the whole problem reduces to find the deformed mid surface such that potential energy is minimized.

3.4.3. Shell Theory

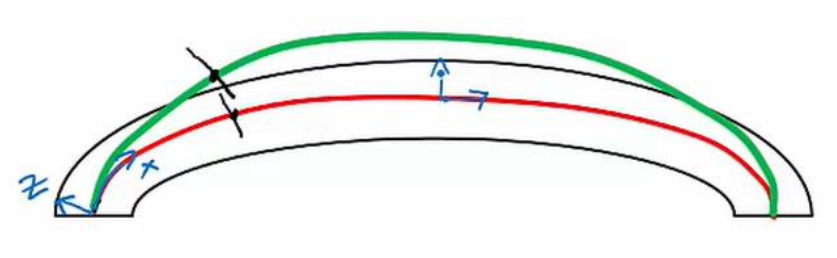

Figure 10: Shell Theory

Shell theory takes the idea of plate theory and extends it to curved surfaces. In this case, we have a structure whose cross- section looks similar to the figure shown above. To visualize the entire structure, take that and extrude it perpendicular to the plane of paper. Again we will focus on the mid surface. Now, the complication is that, unlike the case of a Plate Theory where the mid surface is planar, here it's curved. Under the influence of the load, the mid surface (shown by red line) deforms and becomes something shown by green line. Here, we assume that points on the mid surface moves mostly in the normal direction. So the displacement normal to the surface is the critical one. We need to know the rotation, which comes from the slope of the deformed curve for which the coordinate system has to be curvilinear. Here, X is along the mid line curve (red line), and Z is the direction perpendicular to that midline. All the equations has to be written in terms of these body-fitted coordinate system.

The mathematical details are extremely complex, but fortunately we have a fancy calculator, ANSYS, at our disposal that will take care of the details and so we can focus on solving a very sophisticated problem with a conceptual understanding of how the mathematical model works.

3.5. Material Selection

One of the main objectives of project work is to find out suitable material for windmill blade. Usually the blade used is fiber-reinforced material. The material used for the current experiment are structural steel, Epoxy carbon, E-glass, S-glass, Aluminium alloy.

3.5.1. Aluminum Alloy

Aluminium have been mostly used in aerospace manufacturing mainly due to high strength to weight ratio. Aluminium alloy typically have an elastic modulus of 70GPa, which is about one third of elastic modulus of steel and steel alloy it has high tensile strength, weld ability and corrosion resistance.

Table 4: Material Properties of Aluminium Alloy

S NO.	Property	Value	Unit
1	Density	2770	Kg/m^3
2	Young's Modulus	7.10E+10	Pa
3	Poisson's Ratio	0.33	
4	Bulk Modulus	6.96E+10	Pa
5	Shear Modulus	2.67E+10	Pa
6	Tensile Yield Stress	2.80E+08	Pa
7	Compressive Yield Stress	2.80E+08	Pa
8	Tensile Ultimate Stress	3.10E+08	Pa
9	Compressive Ultimate Stress	0	Pa

3.5.2. E-Glass

E-glass (i.e., borosilicate glass called “electric glass” or “E-glass” for its high electric resistance) Family of glassed with a calcium aluminium borosilicate composition and a maximum alkali composition of 2%.these are used when strength and high electrical resistivity are required.

Table 5: Material Properties of E-Glass

S NO.	Property	Value	Unit
1	Density	2600	Kg/m^3
2	Young's Modulus	7.30E+10	Pa
3	Poisson's Ratio	0.22	
4	Bulk Modulus	4.35E+10	Pa
5	Shear Modulus	2.99E+10	Pa

3.5.3. Epoxy Carbon Woven

In this composite carbon acts as a high performance fiber material, because it has highest specific modulus and high specific strength of all reinforcing fiber material. CFRC is a strong, light and very expensive material. It is extensively used in racing cars. High cost of this material is compensated by its excellent strength to weight ratio.

Table 6: Material Properties of Epoxy Carbon Woven

S NO.	Property	Value	Unit
1	Density	1480	Kg/m^3
2	Young's Modulus X	9.81E+10	Pa
3	Young's Modulus Y	9.81E+10	Pa
4	Young's Modulus Z	9.00E+09	Pa
5	Poisson's Ratio XY	0.05	
6	Poisson's Ratio YZ	0.3	
7	Poisson's Ratio XZ	0.3	
8	Shear Modulus XY	1.95E+10	Pa
9	Shear Modulus YZ	3.00E+09	Pa
10	Shear Modulus XZ	3.00E+09	Pa

3.5.4. S-Glass

S-glass (i.e. high strength glass, S means "Strength" here) developed in the 1960s for military applications, has 40% higher tensile and flexural strengths, and 10...20% higher compressive strength and flexural modulus, than the E-Glass. It contain magnesium alumina silicate mostly used where high strength, high stiffness, extreme temperature resistance and corrosive resistance is needed.

Table 7: Material Properties of S-Glass

S NO.	Property	Value	Unit
1	Density	2500	Kg/m^3
2	Young's Modulus	9.00E+10	Pa
3	Poisson's Ratio	0.22	
4	Bulk Modulus	5.36E+10	Pa
5	Shear Modulus	2.99E+10	Pa
6	Tensile Yield Stress	3.69E+10	Pa

3.5.5. Structural Steel

Table 8: Material Properties of Structural Steel

S NO.	Property	Value	Unit
1	Density	7850	Kg/m^3
2	Young's Modulus	2.00E+11	Pa
3	Poisson's Ratio	0.3	
4	Bulk Modulus	1.67E+11	Pa
5	Shear Modulus	7.69E+10	Pa

Chapter 4 : Results and Discussions

4.1. Results From CFD

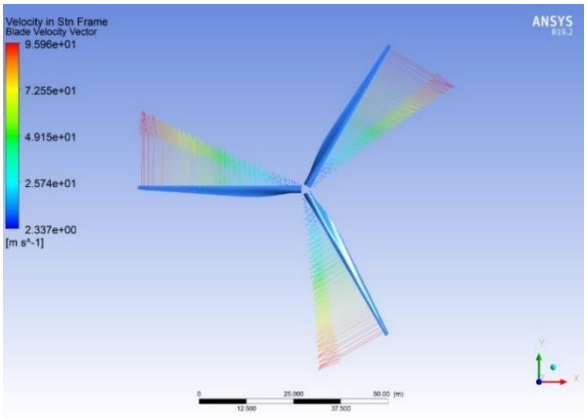

Figure 11: Blade Velocity Vectors

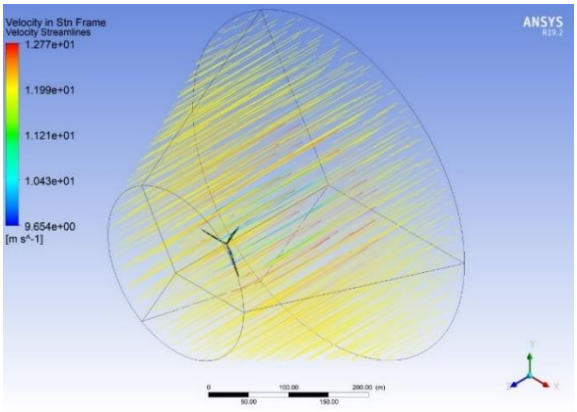

Figure 12: Velocity Streamlines

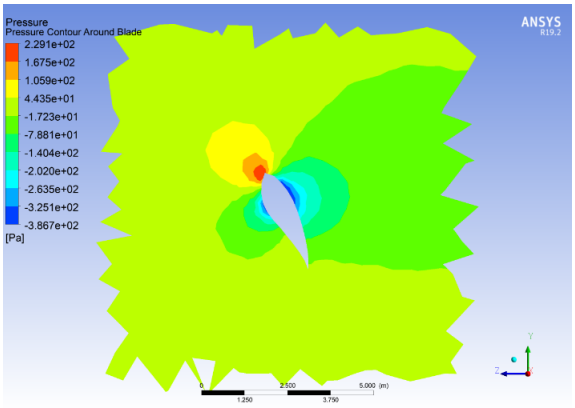

Figure 13: Pressure Contours Around Blade

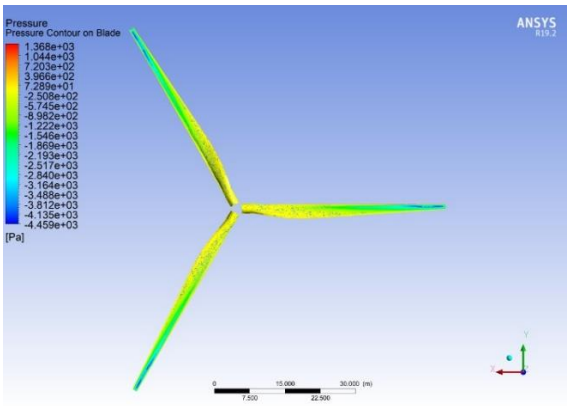

Figure 14: Pressure Contours Downstream

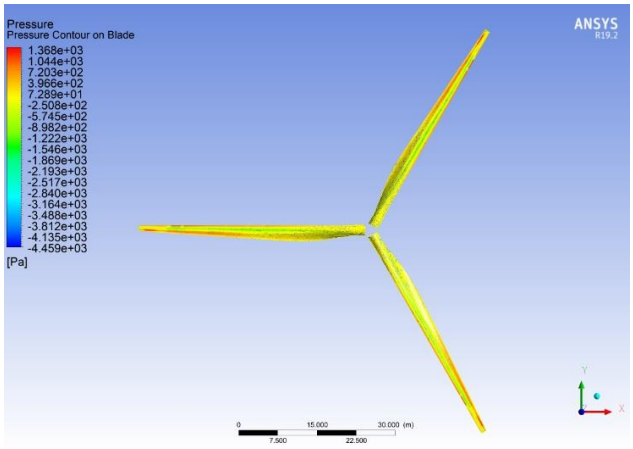

Figure 15: Pressure Contours Upstream

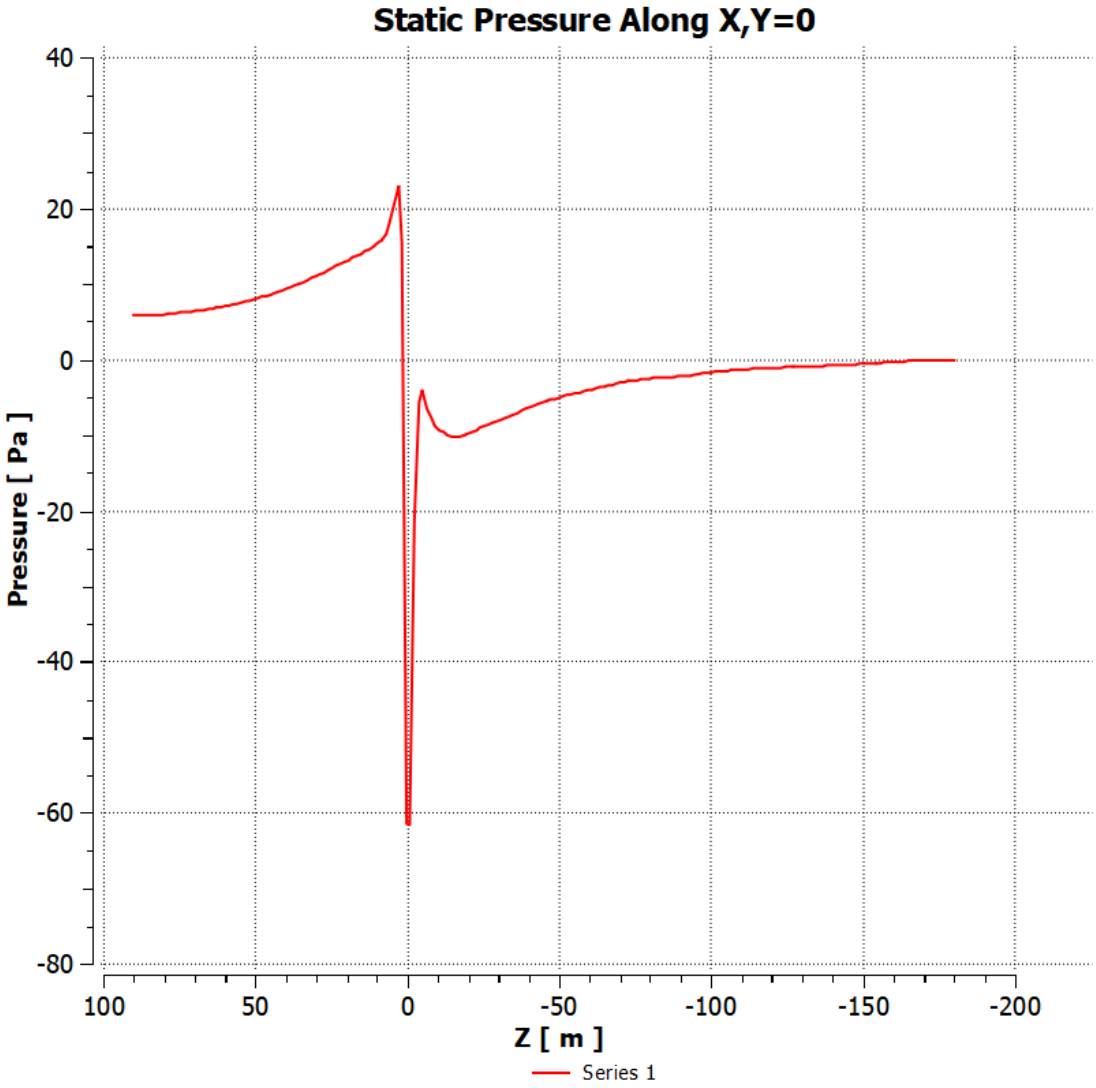

Figure 16: Pressure Variation Along Rotational Axis (Z-Axis)

4.2. Results From FEA

4.2.1. Analysis Using Aluminium Alloy as Blade Material

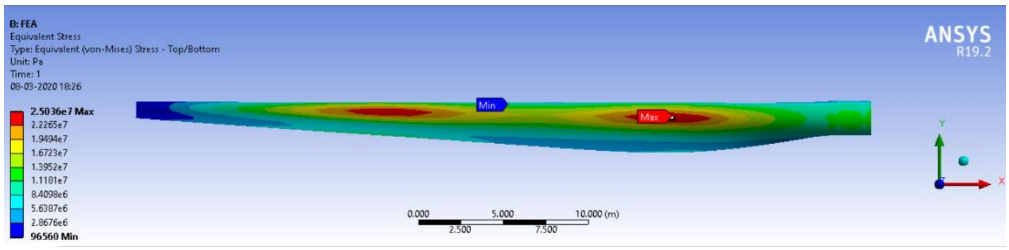

Figure 17: Von-Mises Stress Distribution of Aluminium

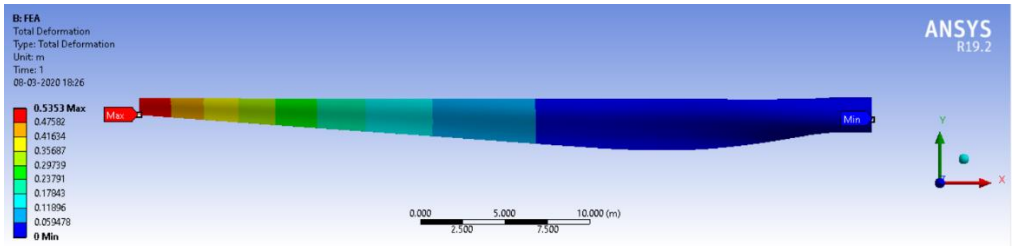

Figure 18: Total Deformation of Aluminium Alloy

4.2.2. Analysis Using E-Glass as Blade Material

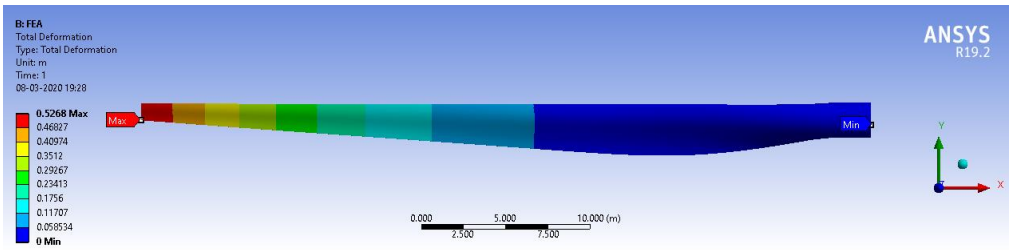

Figure 19: Total Deformation of E-Glass

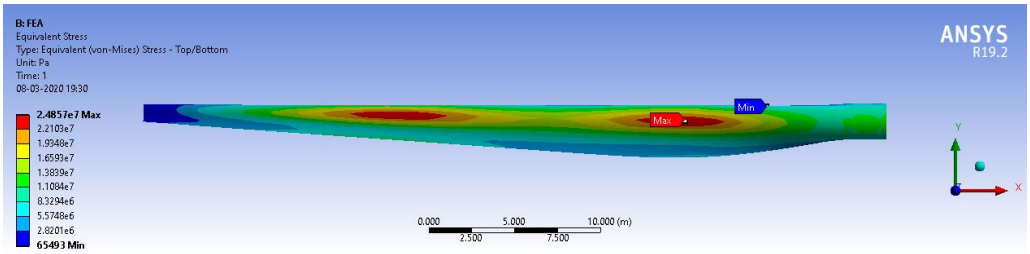

Figure 20: Von-Mises Stresses of E-Glass

4.2.3. Analysis Using Epoxy Carbon Woven as Blade Material

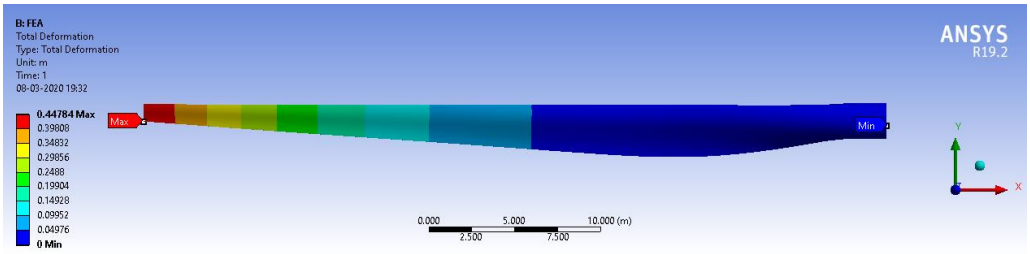

Figure 21: Total Deformation of Epoxy Carbon Woven

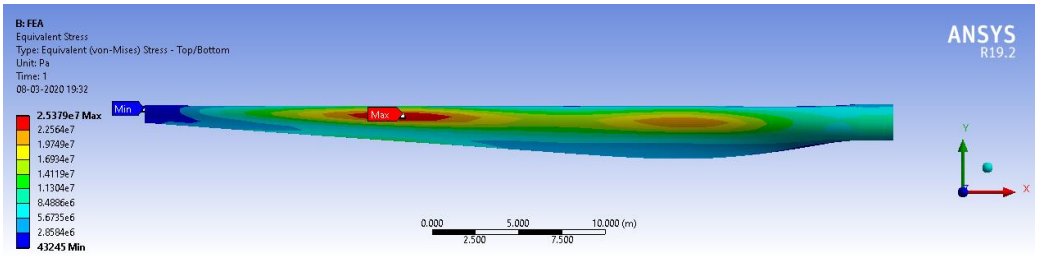

Figure 22: Von-Mises Stresses of Epoxy Carbon Woven

4.2.4. Analysis Using S-Glass as Blade Material

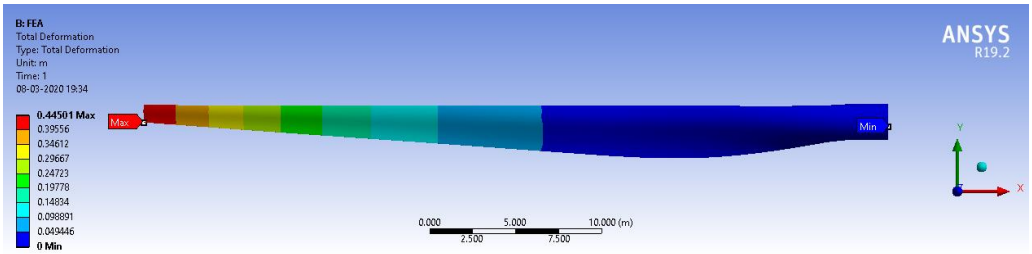

Figure 23: Total Deformation of S-Glass

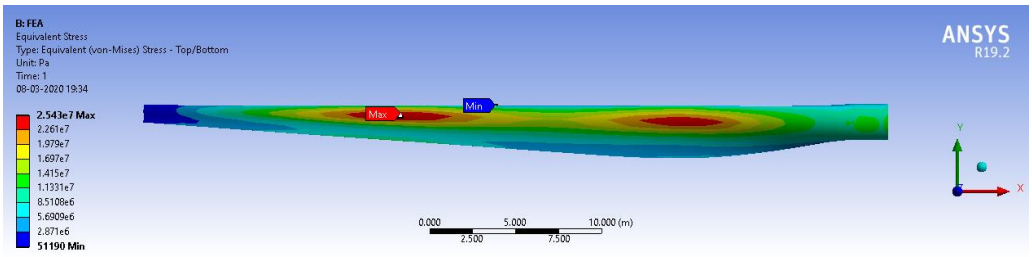

Figure 24: Von-Mises Stresses of S-Glass

4.2.5. Analysis Using Structural Steel as Blade Material

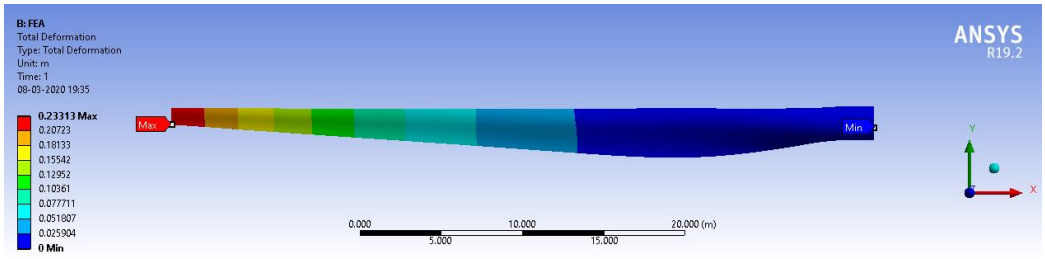

Figure 25: Total Deformation of Structural Steel

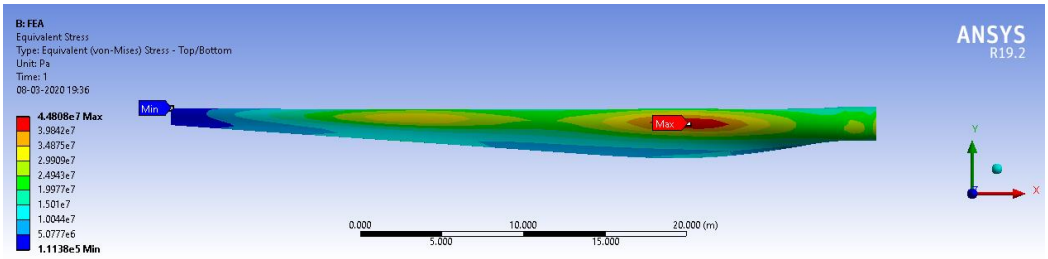

Figure 26: Von-Mises Stresses of Structural Steel

4.2.6. Analysis Using Homogenized Orthotropic Material as Blade Material

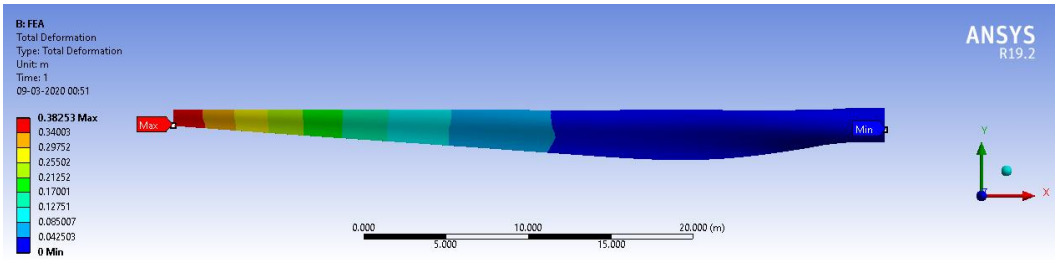

Figure 27: Total Deformation of Homogenized Orthotropic Material

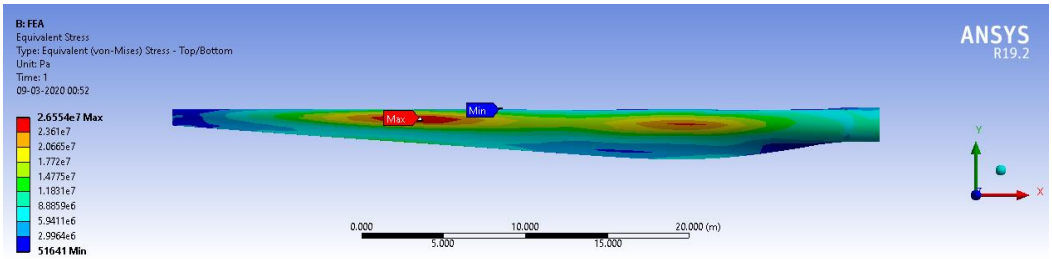

Figure 28: Von-Mises Stresses of Homogenized Orthotropic Material

4.3. Result Table

Table 9: FEA Results

S NO.	Materials	Total Deformation (m)		Von Mises Stress (MPa)		
		Max	Avg	Max	Min	Avg
1	Aluminium Alloy	0.5353	0.1302	25.04	0.0965	7.479
2	E-Glass	0.5268	0.1275	24.857	0.0655	7.474
3	Epoxy Carbon Woven	0.447	0.105	25.379	0.0432	7.409
4	S-Glass	0.445	0.107	25.43	0.0512	7.683
5	Structural Steel	0.233	0.0603	44.81	0.111	12.138

4.4. Effect of Varying Blade Angle

The standard design of our simulation process has the blade angle of 2.7^{o} but in order to find out the optimum performance of these blades if other factors have to be constant we need to vary the blade angles & then by simulating we will get the optimum blade angle. The blade angle that we have taken here is a representation for section at the tip of the blade.

A comparison of performances under different blade angles are given below [15]. One reason for the less number of angle variation in the table is due to the fact that varying the blade angle to more than a limit will get the value of lift coefficient to be negative which is not possible because the air is flowing in negative z-direction which only allows the blade to move in clockwise direction but if the lift is negative than the blade will move in counter clockwise direction theoretically.

Table 10: Effect of Varying Blade Angle on Blade Performance

Blade Angle, ß	Lift, L (N)	Drag, D (N)	Torque, T (N-m)	C_L	C_D	C_L/C_D
2.7	5428.4	82413.5	123433	0.0125	0.19	0.0657
4.7	6673.94	100954	148595	0.0154	0.233	0.066
6.7	5663.13	114322	92668.5	0.013	0.264	0.049

When angle is 6.7^o, the orientation of blade is such that the incoming free stream wind strikes on blade nearly perpendicular to the tip section of the wind turbine blade. Therefore, the blade at this angle gives a reduced value of $\mathbf{C_L/ C_D}$ and so the torque value (see Figure 19 & 22).

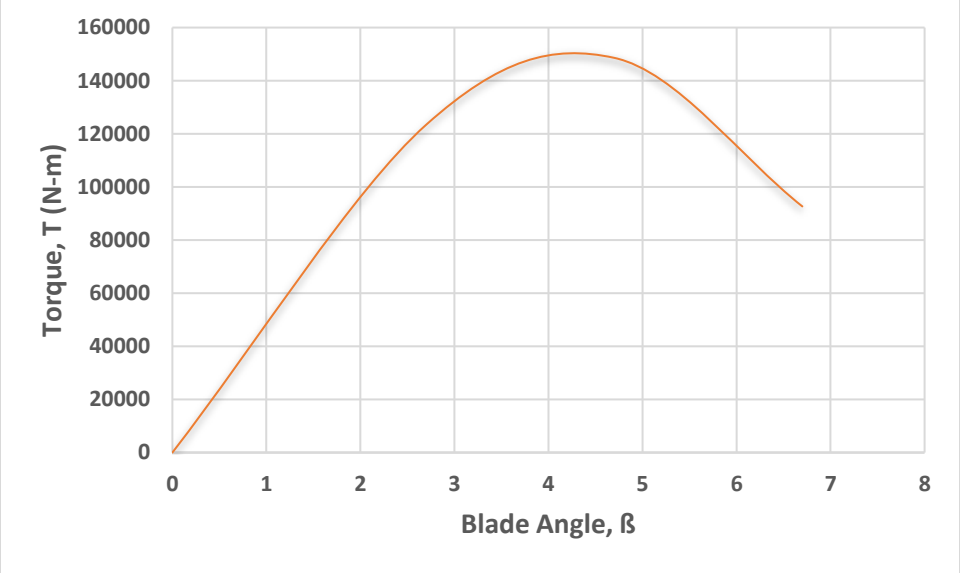

Figure 29: Variation of Torque with Blade Angle

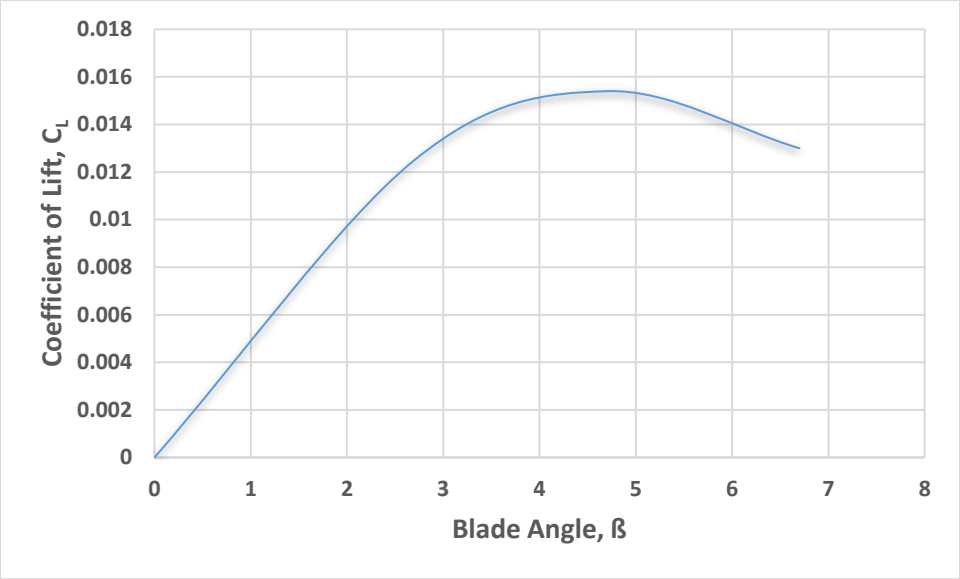

Figure 30: Variation of Coefficient of Lift with Blade Angle

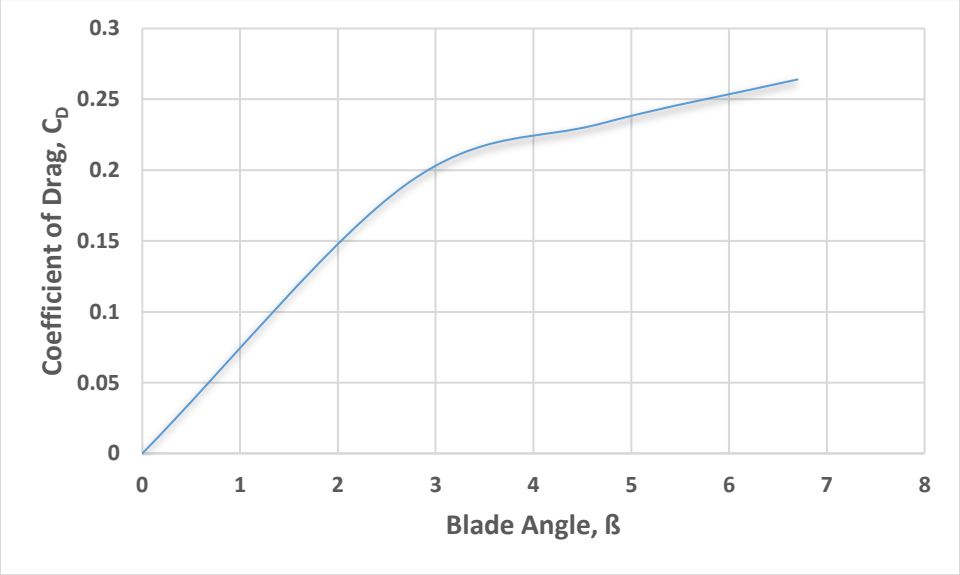

Figure 31: Variation of Coefficient of Drag with Blade Angle

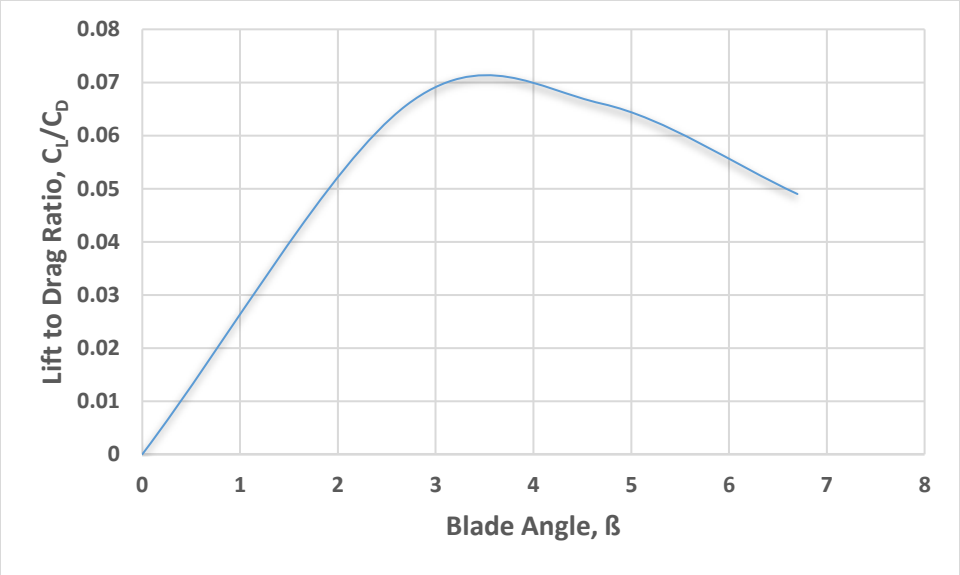

Figure 32: Variation of Lift to Drag Ratio with Blade Angle

Chapter 5 : Conclusion

5.1. Conclusion

In this project, we have analyzed the model by applying two steps. The first part is for CFD, and FEA for the second part. The first part of this project focus on the CFD, which includes many steps like geometry modeling, mesh generation and finally getting the results for the Horizontal Axis Wind Turbine (HAWT). The results which we are getting by the software are very close to the hand calculations. Their validation has also been done to get the results correct. The model should be made properly and their standards must be reviewed.

In the second part of the project, the design and static analysis of composite wind turbine blade had been carried out. The comparison between different composite materials is made under the same loading condition. Properties like stress, strain, and deformation are calculated using ANSYS. The results obtained from ANSYS imply that Epoxy Carbon Woven and E-Glass show overall the least value in stress and Structural Steel in total deformation. This concludes that Epoxy Carbon Woven is more suitable in making a wind turbine blade.

Chapter 6 : References

6.1. References

[1] P. J. Schubel and R. J. Crossley, "Wind Turbine Blade Design," *Energies*, vol. 5, no. 9, pp. 3425–3449, Sep. 2012, doi: 10.3390/en5093425.

[2] M. Fatehi, M. Nili-Ahmadabadi, O. Nematollahi, A. Minaiean, and K. C. Kim, "Aerodynamic performance improvement of wind turbine blade by cavity shape optimization," *Renew. Energy*, vol. 132, pp. 773–785, Mar. 2019, doi: 10.1016/j.renene.2018.08.047.

[3] D. I. Chortis, *Structural analysis of composite wind turbine blades: nonlinear mechanics and finite element models with material damping*. Cham: Springer, 2013.

[4] S. Jaiswal and G. L. Pahuja, "Effect of reliability of wind power converters in productivity of wind turbine," in *2014 IEEE 6th India International Conference on Power Electronics (IICPE)*, Kurukshetra, India, Dec. 2014, pp. 1–6, doi: 10.1109/IICPE.2014.7115791.

[5] V. L. Okulov and J. N. Sørensen, "Maximum efficiency of wind turbine rotors using Joukowsky and Betz approaches," *J. Fluid Mech.*, vol. 649, pp. 497–508, Apr. 2010, doi: 10.1017/S0022112010000509.

[6] G. A. M. van Kuik, "The Lanchester–Betz–Joukowsky limit," *Wind Energy*, vol. 10, no. 3, pp. 289–291, May 2007, doi: 10.1002/we.218.

[7] M. Chandrala, A. Choubey, and B. Gupta, "Aerodynamic Analysis of Horizontal Axis Wind Turbine Blade," *IJERA*, vol. 2, no. 6, p. 5, Dec. 2012.

[8] W. Z. Shen, M. O. L. Hansen, and J. N. Sørensen, "Determination of the angle of attack on rotor blades," *Wind Energy*, vol. 12, no. 1, pp. 91–98, Jan. 2009, doi: 10.1002/we.277.

[9] R. Sathyanarayanan, S. Muthamizh, C. Giriramprasath, and K. T. Gopinath, "Highway windmill," in *2011 IEEE 3rd International Conference on Communication Software and Networks*, Xi'an, China, May 2011, pp. 343–347, doi: 10.1109/ICCSN.2011.6014909.

[10] M. H. Ali, "Experimental comparison study for Savonius wind turbine of two & three blades at low wind speed," *Int. J. Mod. Eng. Res. IJMER*, vol. 3, no. 5, pp. 2978–2986, 2013.

[11] H. P. Gohil and S. T. Patel, "Design procedure for Lenz type vertical axis wind turbine for urban domestic application," *Int. J. Sci. Res. Dev.*, vol. 2, no. 3, pp. 1609–1613, 2014.

[12] O. Pabut, G. Allikas, H. Herranen, R. Talalaev, and K. Vene, "Model validation and structural analysis of a small wind turbine blade," in *8th International DAAAM Baltic Conference, Tallinn, Estonia*, 2012.

[13] C. Phelps and J. Singleton, "Wind turbine blade design," *Ithaca NY*, 2015.

[14] D. J. Malcolm and A. C. Hansen, *WindPACT Turbine Rotor Design Study: June 2000--June 2002*. National Renewable Energy Laboratory, 2006.

[15] B. S. Patil and H. R. Thakare, "Computational Fluid Dynamics Analysis of Wind Turbine Blade at Various Angles of Attack and Different Reynolds Number," *Procedia Eng.*, vol. 127, pp. 1363–1369, 2015, doi: 10.1016/j.proeng.2015.11.495.

[16] GE1.5XLE wind turbine brochure

[17] "Guide To Modeling And Manufacturing Composite Wind Turbine Blades", Cornell iversity, MAE 4021 Project guide, Rev.10/29/2013.